Crystal Structures and Magnetic Properties of *m*-Phenylenebis(imidazole) Derivatives Having Two Nitronyl Nitroxide or Iminyl Nitroxide Radicals. The Two Kinds of Antiferromagnetic Interaction Alternating along One-Dimensional Chains

Ryuji Akabane, Masakazu Tanaka, Kenji Matsuo, and Noboru Koga*

Faculty of Pharmaceutical Sciences, Kyushu University, Fukuoka, 812-82 Japan

Kenji Matsuda and Hiizu Iwamura*

Institute for Fundamental Research of Organic Chemistry, Kyushu University, Fukuoka, 818-81 Japan

Received August 4, 1997[⊗]

1,3-Bis{2-(1-oxyl-3-oxo-4,4,5,5-tetramethylimidazolin-2-yl)imidazol-1-yl}benzene (**1**), 1,3-bis{2-(1-oxyl-4,4,5,5-tetramethylimidazolin-2-yl)imidazol-1-yl}benzene (**2**), and their chloro derivatives (**3** and **4**) were prepared. Both diradicals **1**, **2** and **3**, **4** crystallized in orthorhombic, space group *Pbcn* and in monoclinic, space group $P2_1/c$, respectively. The molecular structures of diradicals **1** and **2** were similar to each other and had C_2 symmetry. Intra- and intermolecular average distances between the two NO groups of the nitronyl nitroxide (NN) moieties in **1** and those of the N−N and NO−NO of the iminyl nitroxide (IN) moieties in **2** were found to be 4.26 and 3.49 Å for **1** and 4.38 and 3.54 Å for **2**, respectively, suggesting the formation of magnetically linear chain structures along the *c* axis. An alternating antiferromagnetic one-dimensional chain model ($H = -2J\Sigma\{S_{A2i}S_{A2i-1} + \alpha S_{A2i}S_{A2i+1}\}$) was applied to the spin systems **1** and **2** and a theoretical equation derived therefrom was fitted to the observed $\chi_{mol}T$ vs T plots to give the exchange coupling parameters, $J/k_B = -158 \pm 2$ and -239 ± 8 K and $\alpha = 0.22 \pm 0.02$ and 0.11 ± 0.04, respectively. The molecular structures of **3** and **4** were also similar to each other, in which two NN and IN groups are far away from each other by the nearest intramolecular average distance between radical centers being 4.54 and 4.72 Å for **3** and **4**, respectively. One of the latter has a disorder with respect to the position of the oxygen atom in IN. One of the two NNs and INs in both diradicals had intermolecular short distances between the radical centers in the neighboring molecules; average distances 3.56 Å for **3** and 3.82 Å for **4**, to form magnetic dimer structures. The exchange coupling parameters for **3** and **4** were determined to be $J/k_B = -4.85 \pm 0.15$ and -37.3 ± 0.3 K (one triplet species for the singlet−triplet model; $H = -2JS_1S_2$, and isolated two doublets in a ratio of 1:1), respectively.

Free radicals capable of serving as bridging ligands for magnetic metal ions are recent subjects of great interest in designing and constructing metal−radical hybrid spin systems that exhibit meta-, ferri-, and ferromagnetism depending on the dimension of the extended structure and mode of the exchange interaction. Metal complexes ligated with nitronyl nitroxides (NN),[1] di- and trinitroxides,[2] nitrogen bases carrying free radicals[3] and carbenes[4] and semiquinones[5] are typical examples. For extending and developing these metal−radical systems, it is important to explore new biradicals having two bidentate ligating sites. 1,3-Bis{2-(1-oxyl-3-oxo-4,4,5,5-tetramethylimidazolin-2-yl)imidazol-1-yl}benzene (**1**) and 1,3-bis{2-(1-oxyl-4,4,5,5-tetramethylimidazolin-2-yl)imidazol-1-yl}benzene (**2**) were designed and synthesized in this work. NN- and IN-imidazole groups in **1** and **2**, respectively, are expected to serve as bidentate ligands[6] and interact magnetically to each other through bonds and/or space. We wish to describe the analyses of their crystal structures and the measurements of their magnetic properties by means of EPR spectroscopy and SQUID magneto/susceptometry. Similar studies have been carried out in the corresponding chloro derivatives **3** and **4**.

[⊗] Abstract published in *Advance ACS Abstracts,* November 15, 1997.

(1) (a) Caneschi, A.; Gatteschi, D.; Laugier, J.; Rey, P.; Sessoli, R. *Inorg. Chem.* **1988**, *27*, 1553 (b) Caneschi, A.; Gatteschi, D.; Renard, J. P.; Rey, P.; Sessoli, R. *Inorg. Chem.* **1989**, *28*, 1976. (c) Caneschi, A.; Gatteschi, D.; Rey, P. *Prog. Inorg. Chem.* **1991**, *30*, 331. (d) Caneschi, A.; Chiesi, P.; David, L.; Ferraro, F.; Gatteschi, D.; Sessoli,R. *Inorg. Chem.* **1993**, *32*, 1445. (e) Stumpf, H. O.; Ouahab, L.; Pei, Y.; Grandjean, D.; Kahn, O. *Science* **1993**, *261*, 447.

(2) (a) Ishimaru, Y.; Inoue, K.; Koga, N.; Iwamura, H. *Chem. Lett.* **1994**, 1693. (b) Inoue, K.; Iwamura, H. *J. Chem. Soc., Chem. Commun.* **1994**, 2273. (c) Kitano, M.; Ishimaru, Y.; Inoue, K.; Koga, N.; Iwamura, H. *Inorg. Chem.* **1994**, *33*, 6012. (d) Inoue, K.; Iwamura, H. *J. Am. Chem. Soc.* **1994**, *116*, 3173. (e) Kitano, M.; Koga, N.; Iwamura, H. *J. Chem. Soc., Chem. Commun.* **1994**, 447. (f) Inoue, K.; Hayamizu, T.; Iwamura, H. *Chem. Lett.* **1995**, 745. (g) Inoue, K.; Hayamizu, T.; Iwamura, H. *Mol. Cryst. Liq. Cryst.* **1995**, *273*, 67. (h) Inoue, K.; Hayamizu, T.; Iwamura, H.; Hashizume, D.; Ohashi, Y. *J. Am. Chem. Soc.* **1996**, *118*, 1803. (i) Inoue, K.; Iwamura, H. *Adv. Mater.*, in press. (j) Oniciu, D. C.; Matsuda, K.; Iwamura, H. *J. Chem. Soc., Perkin 2* **1996**, 907. (k) Iwamura, H.; Inoue, K.; Hayamizu, T. *Pure Appl. Chem.* **1996**, *68*, 243.

(3) (a) Eaton, G. R.; Eaton, S. S. *Acc. Chem. Res.* **1988**, *21*, 107. (b) Burdukov, A. B.; Ovcharenko, V. I.; Ikorski, V. N.; Pervukhina, N. V.; Podberezskaya, N. V.; Grigor′ev, I. A.; Larionov, S. V.; Volodarsky, L. B. *Inorg. Chem.* **1991**, *30*, 972.

(4) (a) Koga, N.; Ishimaru, Y.; Iwamura, H. *Angew. Chem., Int. Ed. Engl.* **1996**, *36*, 755. (b) Sano, Y.; Tanaka, M.; Koga, N.; Matsuda, K.; Iwamura H. *J. Am. Chem. Soc.* **1997** *119*, 8246. (c) Karasawa, S.; Tanaka, M.; Koga, N.; Iwamura, H. *J. Chem. Soc., Chem. Commun.* **1997**, 1359.

(5) (a) Caneschi, A.; Dei, A.; Gatteschi, D. *J. Chem. Soc., Chem. Commun.* **1992**, 630. (b) Shultz, D. A.; Boal, A. K.; Driscoll, D. J.; Farmer, G. T.; Kitchin, J. R.; Miller, D. B.; Tew, G. N. *Mol. Cryst. Liq. Cryst.* **1997**, in press.

(6) Yoshioka, N.; Irisawa, M.; Aizawa, N.; Aoki, T.; Inoue, H.; Ohba, S., *Mol. Cryst. Liq. Cryst.* **1996**, *286*, 165.

S0022-3263(97)01438-2 CCC: $14.00

Table 1. Crystal Data and Experimental Parameters of X-ray Crystal Analyses of 1−4

	1	**2**	**3**	**4**
formula	$C_{26}H_{32}N_8O_4$	$C_{26}H_{32}N_8O_2$	$C_{26}H_{31}N_8O_4Cl$	$C_{26}H_{31}N_8O_2Cl$
M	520.59	488.59	555.04	523.04
crystal system	orthorhombic	orthorhombic	monoclinic	monoclinic
space group	P_{bcn}	P_{bcn}	$P2_1/c$	$P2_1/c$
a, Å	10.448(6)	10.617(3)	11.859(2)	11.924(1)
b, Å	13.859(4)	13.082(2)	11.369(2)	11.314(5)
c, Å	18.147(4)	18.371(4)	20.368(2)	20.344(2)
β, deg			95.05(1)	96.191(7)
V, A^3	2627(1)	2551(1)	2735.5(7)	2728.6(9)
Z	4	4	4	4
D, g/cm^3	1.316	1.272	1.348	1.273
no. of observations	436 ($I > 3.00\sigma(I)$)	678 ($I > 3.00\sigma(I)$)	2653 ($I > 3.00\sigma(I)$)	1756 ($I > 3.00\sigma(I)$)
no. of variables	174	165	353	345
$R(I)$	0.049	0.060	0.068	0.069
$R_w(I)$	0.030	0.055	0.060	0.066

Scheme 1

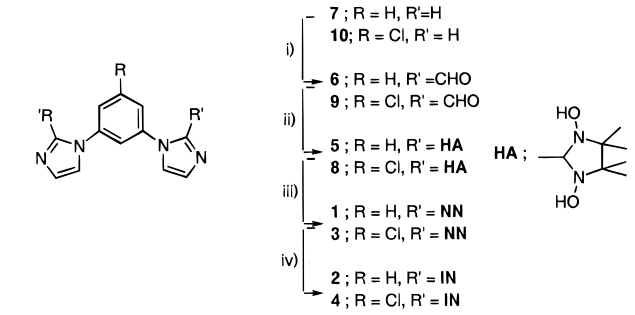

Table 2. Selected Torsion Angles, Bond Angles, Bond Lengths, and Nonbonded Contacts for Biradical 1 and 2

	1		**2**
Torsion Angles, deg			
N1−C1−C8−N4	137		137.1
N1−C1−C8−N3	−44		−47
N2−C1−C8−N4	−46		−45
N2−C1−C8−N3	130		130.1
C8−N4−C12−C11	−38		−33
C8−N4−C12−C13	144		146.6
C10−N4−C12−C11	131		135.4
C10−N4−C12−C13	−44		−45
Bond Angles, deg			
O1−N1−C1	125	O1−N2−C1	126
O1−N1−C2	122	O1−N2−C3	123.8
O2−N2−C1	126		
O2−N2−C3	121		
Bond Lengths, Å			
O1−N1	1.24	O1−N2	1.29
O2−N2	1.27		
Nonbonded Contacts, Å			
O1−O*1	3.97	N1−N*1	4.38
N1−N*1	4.54	O1−O1[a]	3.24
O2−O2[a]	3.22	N2−N2[a]	3.84
N2−N2[a]	3.75		

[a] Intermolecular distance.

Results and Discussions

Preparations of Biradicals. Routes to biradicals **1**−**4** are summarized in Scheme 1. Starting 1,3-di(*N*-imidazolyl)benzene and its chloro derivative were selectively lithiated at position 2 of the imidazole rings with *n*-butyllithium followed by the reaction with *N*,*N*-dimethylformamide to afford diformyl derivatives. Biradicals having NN and IN groups were prepared by a standard procedure[7] reported previously.

The biradicals obtained were very stable in solution and solid states. Biradicals **1**−**4** were obtained by recrystallization as single crystals that were subjected to X-ray crystal and molecular structure analyses.

Crystal Structures. Pertinent crystallographic parameters and refinement data are listed in Table 1. Selected torsion angles, bond angles, bond lengths, and nonbonded contacts are reported in Tables 2 and 3 for biradical **1** and **2**, and for **3** and **4**, respectively.

As shown in the ORTEP drawings for **1** and **2** in Figures 1a and b, respectively, both the radicals have C_2 symmetry axes through C11 and C14 of the benzene ring and have similar molecular structures in which two radical centers are close to each other by twisting the imidazole rings in a disrotatory fashion: the dihedral angles between the phenylene and imidazole ring, and imidazole ring and the radical plane are 36−49 and 43−50° for **1** and 33−45 and 43.9−49.9° for **2**, respectively. Intramolecular through-space average distance ($r_{O1N1-O'1N'1}$) of $r_{O1-O'1}$ and $r_{N1-N'1}$ for **1** and distance ($r_{N1-N'1}$) for **2** are 4.26 and 4.38 Å, respectively. As shown in Figure 2, the crystal structure for both radicals are also similar. The molecules aligned alternatively along the *c* axis with the intermolecular average distance ($r_{O2N2-O2N2}$) between the oxygen and nitrogen atoms of the nitroxide by 3.49 Å for **1** and 3.54 Å for **2**. Taking the short distances ($r_{O1N1-O'1N'1}$ = 4.26 Å and $r_{N1-N'1}$ = 4.38 Å for **1** and **2**, respectively) between the two radical centers within a molecule into account, these radicals in crystals, especially for **1**, are considered to have a magnetically one-dimensional chain structure. The nearest distance of the radical centers between the chains is 5.84 for **1** and 7.74 Å for **2**, indicating that interchain magnetic interaction is less significant.

As observed in ORTEP drawing of Figure 3, the molecular structure of chloro derivatives **3** and **4** are also similar to each other and have no symmetry axis. The two NN and IN groups in a molecule are away from each other and largely twisted toward the imidazole rings; the dihedral angles between the phenylene and imidazole

(7) Ullman, E. F.; Osiecki, J. H.; Boocok, D. G. B.; Darcy, R. *J. Am. Chem. Soc.* **1972**, *94*, 7049.

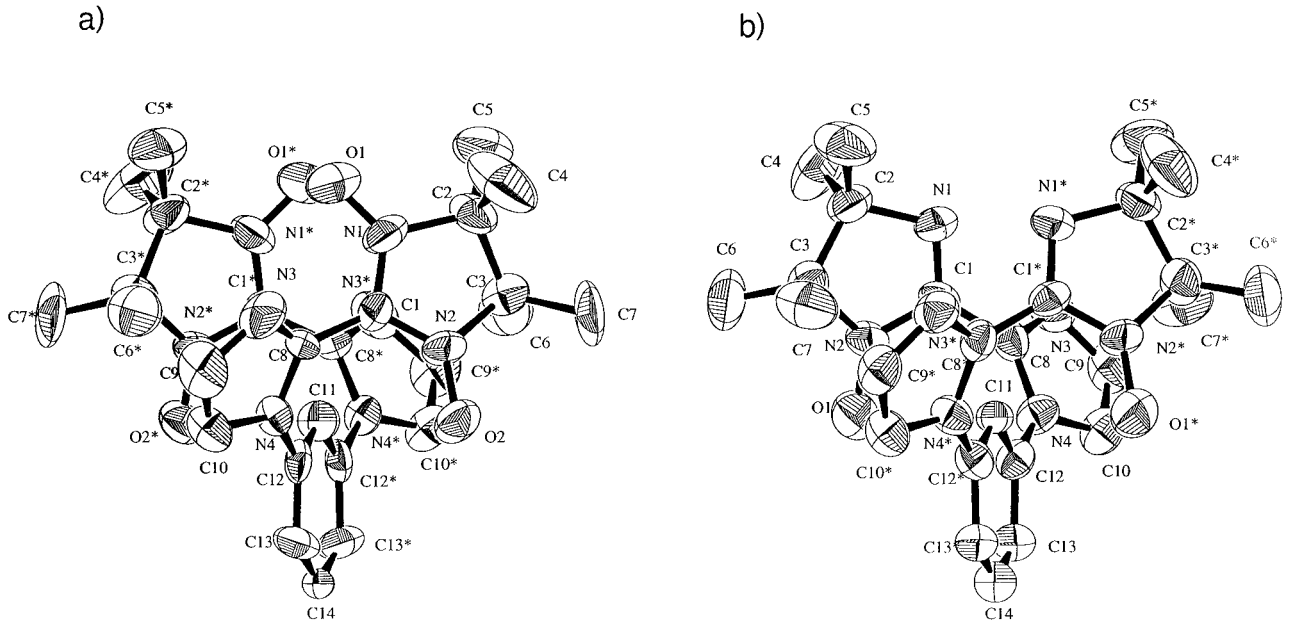

Figure 1. ORTEP drawings of biradicals **1** (a) and **2** (b) (ellipsoids at 30% probability).

Table 3. Selected Torsion Angles, Bond Angles, Bond Lengths, and Nonbonded Contacts for Biradical 3 and 4

	3		**4**
	Torsion Angles, deg		
N1−C7−C10−N3	38.5	N1−C7−C10−N3	36
N1−C7−C10−N4	−133.8	N1−C7−C10−N4	−140.2
N2−C7−C10−N3	−145.1	N2−C7−C10−N3	−151.6
N2−C7−C10−N4	42.6	N2−C7−C10−N4	32
C4−C5−N2−C7	−137.3	C4−C5−N2−C7	−133.7
C4−C5−N2−C9	38.3	C4−C5−N2−C9	39
C6−C5−N2−C7	43.5	C6−C5−N2−C7	46
C6−C5−N2−C9	−140.9	C6−C5−N2−C9	−140.6
N5−C17−C20−N7	67.4	N5−C17−C20−N7	−136
N5−C17−C20−N8	−115.8	N5−C17−C20−N8	46
N6−C17−C20−N7	−109.4	N6−C17−C20−N7	46
N6−C17−C20−N8	67.5	N6−C17−C20−N8	−130
C2−C3−N5−C17	−128.6	C2−C3−N5−C17	−127
C2−C3−N5−C18	53	C2−C3−N5−C18	56
C4−C3−N5−C17	51.2	C4−C3−N5−C17	51
C4−C3−N5−C18	−127.2	C4−C3−N5−C18	−125
	Bond Angles, deg		
O1−N3−C10	126.8	O1−N3−C10	127.4
O1−N3−C11	122.8	O1−N3−C11	123.9
O2−N4−C10	127.3	O2−N7−C20	125
O2−N4−C12	120.6	O2−N7−C21	121
O3−N8−C20	125.9		
O3−N8−C21	122.1		
O4−N7−C20	124.6		
O4−N7−C22	123.4		
	Bond Lengths, Å		
O1−N3	1.27	O1−N3	1.28
O2−N4	1.29	O2−N7	1.26
O3−N8	1.25		
O4−N7	1.26		
	Nonbonded Contacts, Å		
O1−O1[a]	3.30	O1−O1[a]	3.62
N3−N3[a]	3.81	N3−N3[a]	4.01
O4−O2	3.90	N4−N8	4.71
N7−N4	5.18	(N4−O2)	(4.73)
O3−O3[a]	4.04		
N8−N8[a]	5.28		

[a] Intermolecular distance.

rings, and the imidazole ring and the radical plane are 51.2−53 and 64.2−70.6° for the side indicated by dashed square and 38.3−43.5 and 34.9−46.2° for the other, respectively, in **3**. Those dihedral angles are 51−56 and 44−50° for the one and 39.0−46.3 and 28.4−39.8° for the other, respectively, in **4**. Intramolecular through-space average distance ($r_{O2O4-N4N7}$) of r_{O2-O4} and r_{N4-N7} for **3** is 4.54 Å. One of the two INs in **4** indicated by dashed square in Figure 3b is disordered in 1:1 probability and the intramolecular average distances between the radical centers (r_{N4-N8} and $r_{N4-N7O3}$) are 4.71 and 4.72 Å. As indicated in the crystal structure of Figure 4, both radical molecules have the nearest ones in which average intermolecular distances ($r_{O1N3-N1O3}$) between the radical centers are 3.56 Å for **3** and 3.82 Å for **4** to form the dimer structure. The average distances between the nearest radical centers of the dimers are 4.66 and 5.53 Å for **3** and **4**, respectively.

EPR Spectra. EPR spectra of **1**, **2**, **3**, and **4** in 2-methyltetrahydrofuran (MTHF) solution at room temperature consisted of five ($a_N/2$ = 7.26 and 7.17 G for **1** and **3**, respectively) and seven lines ($a_N/4$ = 4.30 and 4.29 G for **2** and **4**, respectively) due to hyperfine coupling with the nitrogen nuclei overlapped with one broad signals at g = 2.0069, 2.0062, 2.0070, and 2.0066, respectively. Ground powder samples showed one broad signal (H_{pp} = 1.46, 3.25, 0.80, and 1.24 mT) at g = 2.009, 2.012, 2.007, and 2.007 for **1**, **2**, **3**, and **4**, respectively.

EPR spectra (ν_0 = 9.411 GHz) in frozen MTHF solutions were obtained in the temperature range 10−100 K. All the four EPR spectra contained two sets of signals characteristic of triplet species at ca. g = 2.00 in addition to the signals due to $\Delta m_S = \pm 2$ transitions. The spectrum of **1** at 10 K is shown in Figure 5a as an example and was simulated[8] (Figure 5b) by a sum of two triplet spectra in a 1:4 ratio with zero-field splitting parameters $|D/hc|$ = 0.00726, 0.00270 and $|E/hc|$ = 0.00002, 0.00002 cm^{-1}, respectively.

The intramolecular average distances between the radical centers were estimated to be 7.1 Å by applying a point dipole approximation to the former $|D/hc|$ value (0.00726 cm^{-1}). This value is different from the intramolecular through-space distance of 4.26 Å revealed by X-ray analysis, suggesting that the molecular structure

(8) The simulation of the EPR fine structure was performed by using a program based on the second-order perturbation theory and provided by Professors K. Ito and T. Takui of Osaka City University.

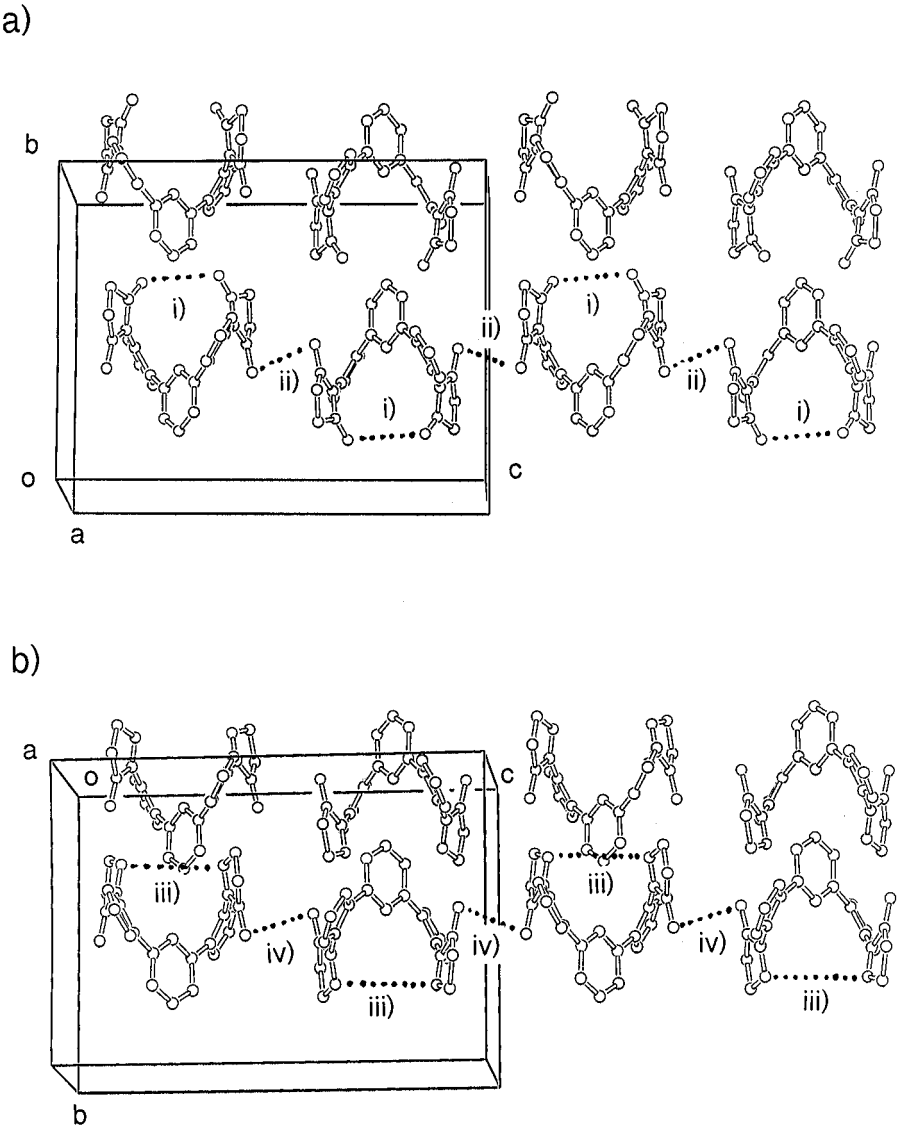

Figure 2. Views of the unit cell of biradicals **1** (a) and **2** (b). Methyl groups have been omitted for the sake of clarity. Average distances between the radical centers: (i) 4.26 Å, (ii) 3.49 Å, (iii) 4.38 Å, and (iv) 3.54 Å.

in frozen solution and in crystalline state might be different and the former may not be unique but consist of at least two conformers (rotamers). Similarly, the triplet spectra for the other biradicals were interpreted not by single species but two conformers with different composition. The two radical centers in these molecules interact magnetically to each other through-space and/or through-bond to produce triplet species. The intensities (I) of the observed triplet signals linearly decreased with increasing temperature (T) from 13 to 100 K in I vs T^{-1} plot; the temperature dependence of triplet signal intensities suggested either that triplet states are ground states or they are degenerate with singlet states.

Magnetic Susceptibility. The paramagnetic susceptibilities of microcrystalline samples were measured at 2−350 K for **1** and **2**, and 2−300 K for **3** and **4** at a constant field of 500 mT. Temperature dependence of the molar paramagnetic susceptibility χ_{mol} was obtained and presented as $\chi_{mol}T$ vs T plots for biradicals **1** and **2** and their chloro derivatives **3** and **4** in Figures 6 and 7, respectively.

(A) Biradical 1 and 2. $\chi_{mol}T$ values of 0.651 and 0.613 emu·K·mol^{-1} at 350 K for **1** and **2**, respectively, are already smaller than those of 0.751 emu·K·mol^{-1} calculated for a spin only value either of two isolated $S = 1/2$ or degenerate singlet−triplet spin systems. As the temperature was lowered from 350 K, $\chi_{mol}T$ values for **1** and **2** decreased gradually to nearly zero at ca. 30 and 50 K, respectively, as shown in Figure 6. The observed thermal behavior of $\chi_{mol}T$ values for both samples indicates that strong antiferromagnetic interactions took place in crystalline states and that their magnitude was greater for **2** than **1**.

Scheme 2

$$\text{----- } S_{A2i-1} \underset{\alpha J}{\text{——}} S_{A2i} \underset{J}{\text{——}} S_{A2i+1} \underset{\alpha J}{\text{-----}} \underset{J}{}$$

To understand these magnetic interactions quantitatively, an antiferromagnetic alternating one-dimensional chain model[9,10] (Scheme 2) suggested by the X-ray crystal structure data (Figure 2) was applied to the spin systems of radicals **1** and **2**, in which intramolecular through-bond interaction were insignificant by large dihedral angles

(9) (a) Duffy, W.; Barr, K. P. *Phys. Rev.* **1968**, 165, 647. (b) Hall, J. W.; Marsh, W. E.; Weller, R. R.; Hatfield, W. E. *Inorg. Chem.* **1981**, *20*, 1033.

(10) Kahn, O. *Molecular Magnetism*; VCH: New York, 1993; Chapter 11.

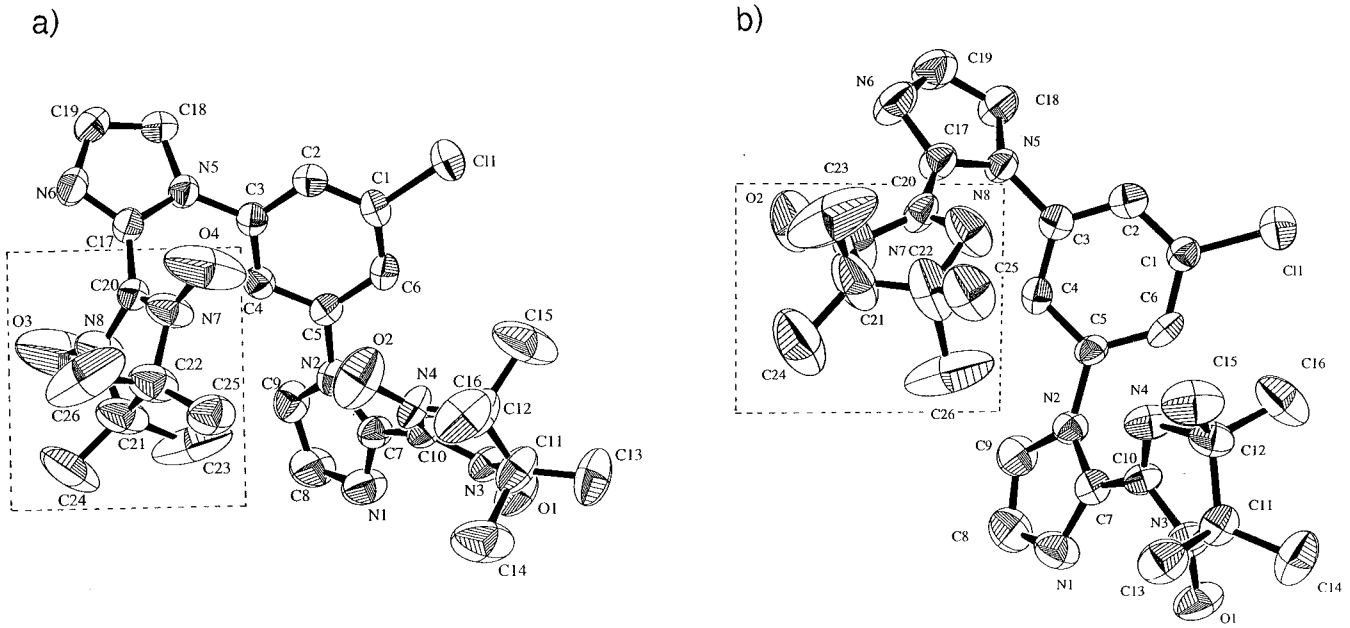

Figure 3. ORTEP drawings of biradicals **3** (a), and **4** (b) (ellipsoids at 30% probability).

between the benzene and imidazole rings, and the imidazole and radical units.

The spin Hamiltonian for such systems is given by

$$H = -2J\Sigma\{S_{A2i}S_{A2i-1} + \alpha S_{A2i}S_{A2i+1}\} \qquad (1)$$

where α is an alternation parameter smaller than unity. The equations[9] derived from the eigenvalues of this Hamiltonian for $0 < \alpha < 0.4$ and $0.4 < \alpha$ were fitted to the experimental data from 350 to 2 K. For the fitting, g value of 2.009 and 2.012 for **1** and **2**, respectively, obtained from EPR spectra of their ground samples were employed. Although theoretical curves slightly deviated from experimental data in the low-temperature region, the best fit parameters; $J/k_B = -158 \pm 2$, -239 ± 8 K, and $\alpha = 0.22 \pm 0.02$, 0.11 ± 0.04 for **1** and **2**, respectively, were obtained. The best-fit curves are shown in Figure 6 as solid curves. Taking the distance between the radical centers in crystal structures of **1** and **2** into account, we find that the J and αJ values are due to the inter- (J_{inter}) and intramolecular (J_{intra}) through-space interactions; $J_{inter}/k_B = -158$, -239 K and $J_{intra}/k_B = -34.8$, -26.3 K for **1** and **2**, respectively. The difference in the α values between **1** and **2** was explained by assuming that the spins in biradical **2** are mainly localized on the N−O atoms in IN moieties[11] in addition to that the intermolecular distance between N−N of IN in a molecule **2** is slightly longer than the one of NO−NO in **1** ($r_{N1-N'1} = 4.38$ Å for **2** and $r_{O1N1-N'1O'1} = 4.26$ Å for **1**).

(B) Biradical 3 and 4. As shown in the $\chi_{mol}T$ vs T plot for biradical **3** (Figure 7a), $\chi_{mol}T$ values above 60 K are constant at 0.74 emu·K·mol^{-1} and those below 60 K decreased with decreasing temperature. The observed $\chi_{mol}T$ vs T profile showed an ordinary antiferromagnetic interaction. On the other hand, the $\chi_{mol}T$ values of biradical **4** decreased gradually from 300 to 20 K and in a slightly stepwise manner below 20 K as temperature was decreased (Figure 7b). The step-shaped decrease cannot be explained by a simple S−T model but suggests either the presence of a high-spin state with a considerably large energy gap to the next lower state or a mixture of species having two different negative J value, one large and the other small.

The crystal structures (Figure 4a,b) of **3** and **4** suggest two kinds of spin models: a combination of the singlet−triplet model ($H = -2J(S_1S_2)$) and the isolated doublet model in a ratio of 1:1 on one hand, and a four-spin model which depends on the presence or absence of the intramolecular interaction on the other. The experimental data were fitted by Bleaney−Bowers equation[12] (S−T model) plus an isolated doublet term to give $g = 1.966 \pm 0.003$, 1.930 ± 0.020, $J/k_B = -4.85 \pm 0.15$, -37.3 ± 0.3 K, $\theta = 0$, -0.45 ± 0.02 K for **3** and **4**, respectively. The best-fit curves are shown in Figure 7 as solid curves. When intramolecular interactions are significant, their spin system become four spin linear chain ($H = -2J(S_1S_2 + S_3S_4) - 2\alpha J(S_2S_3)$, where J and αJ mean intra- and intermolecular exchange coupling constants, respectively). Theoretical equations[13] were fitted to the experimental data by means of a least-squares method to give the best fitted parameters: $g = 1.970 \pm 0.003$, 1.932 ± 0.02, $J/k_B = -0.95 \pm 0.40$, -0.27 ± 0.30 K, $\theta = 0$, -0.46 ± 0.03 and $\alpha = 4.05 \pm 2.31$, 136 ± 152, for **3** and **4**, respectively. The obtained intramolecular J/k_B values are very small indicating that intramolecular through-space interaction (4.54 and 4.72 Å for **3** and **4**, respectively) was insignificant.

Comparisons of J_{inter}/k_B Values between Biradicals 1, 2 and 3, 4. Intermolecular J_{inter}/k_B values obtained by fitting theoretical equations to the experimental data and the average distances between radical centers revealed by X-ray analysis for four biradicals are summarized in Table 4.

The magnitude of the J/k_B values are considerably different in unsubstituted biradicals **1** and **2** and their chloro derivatives **3** and **4**, while their intermolecular average distances between the radical centers are nearly

(11) Akita, T.; Mazaki, Y.; Kobayashi, K.; Koga, N.; Iwamura, H. *J. Org. Chem.* **1995**, *60*, 2092.

(12) Bleaney, B.; D. Bowers, K. *Proc. R. Soc. London* **1952**, *A214*, 451.

(13) Mitsumori, T.; Inoue, K.; Koga, N.; Iwamura, H. *J. Am. Chem. Soc.* **1995**, *117*, 2467.

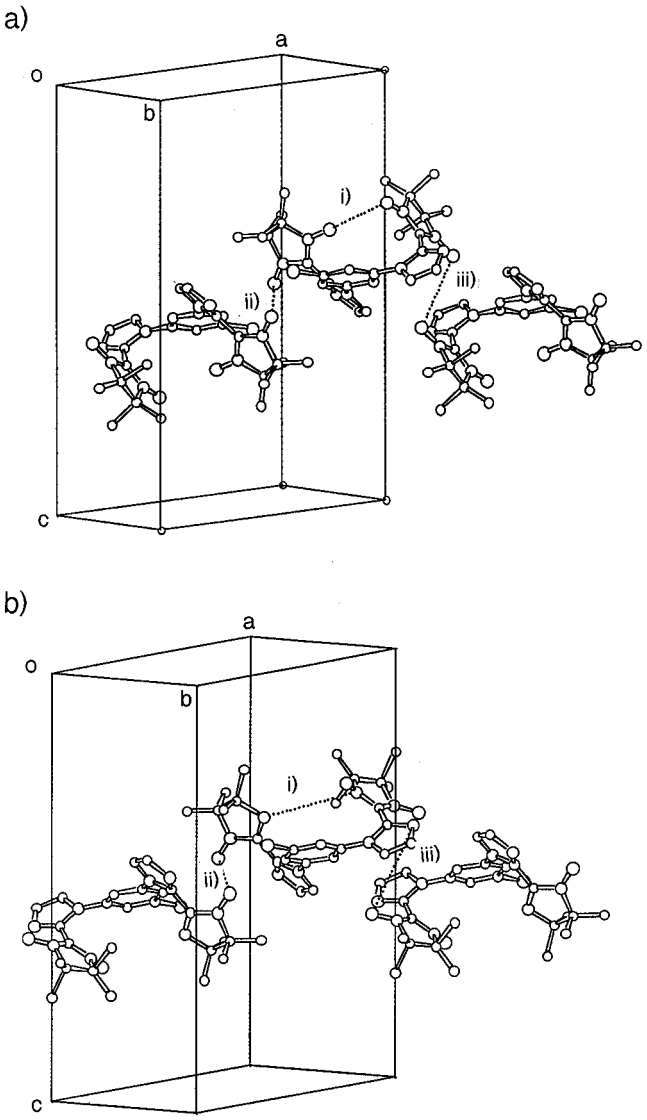

Figure 4. View of the crystal structure of biradical **3** (a) and **4** (b). Average distances between the radical centers: (i) 4.54 and 4.72 Å, (ii) 3.56 and 3.82 Å, (iii) 4.66 and 5.53 Å for **3** and **4**, respectively.

Table 4. Intermolecular Exchange Parameters ($-J_{inter}/K_B$) and Distances for Biradical 1−4

	1	**2**	**3**	**4**
$-J_{inter}/k_B$ (K)	158	239	4.85	37.3
distances (Å)[a]	3.49	3.54	3.56	3.83

[a] Intermolecular average distances between radical centers.

equal (slightly longer in **1** and **2** than in **3** and **4**). These NO−NO short contacts were also observed in the crystal structure of imidazole,[14] 1-methylimidazole,[15] *N*-methylpyridine[16] derivatives having NN groups at position 2 and produced strong intermolecular antiferromagnetic interactions between the NNs. Although those observed in this work were also considered to be caused by short NO−NO contact, this large difference in the J_{inter}/k_B values cannot be explained only by the average distances of radical centers. Relative orientation of the radical

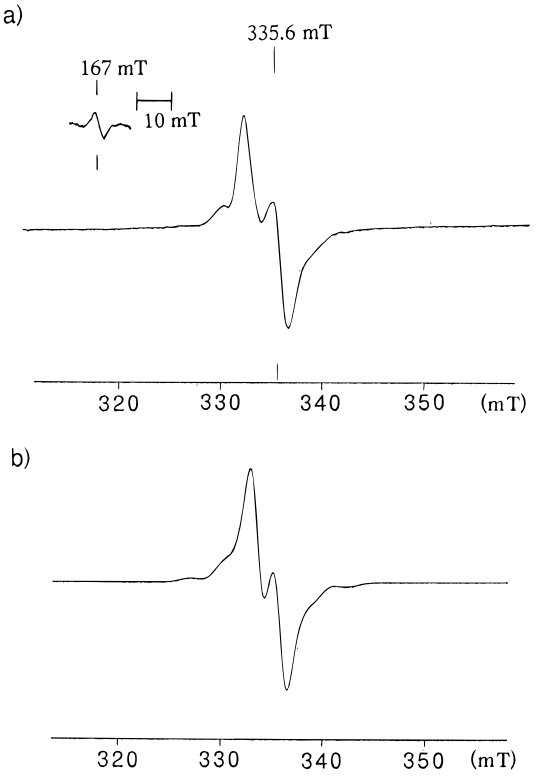

Figure 5. (a) X-band EPR(9.411 GHz) spectrum of **1** in frozen MTHF solution at 10 K. (b) Simulated spectrum of a randomly oriented triplet species for **1**.

centers revealed by X-ray analysis in four biradicals is given in Figure 8 where one set of radical planes of NN and IN unit are found to be nearly parallel to each other and the π-orbitals containing the radical spins take an orthogonal position to the radical plane (to the paper plane).

As seen in Figure 8, the radical center units of biradicals **1** and **2** have the appropriate geometry in which π-orbitals of radical centers overlapped to each other more ideally than those for **3** and **4**. Therefore, they give rise to a large difference in the negative J/k_B values between **1**, **2** and **3**, **4**.

Conclusion

The through-bond interaction between the two radical centers was not dominant due to large dihedral angles between phenylene−imidazole rings and between imidazole−radical planes in crystalline state of biradicals **1**−**4**. Both **1** and **2** have similar crystal structure as well as molecular structure and show alternating antiferromagnetic one-dimensional chain interaction with $J_{inter}/k_B = -158$ K, $J_{intra}/k_B = -35$ K and $J_{inter}/k_B = -239$ K, $J_{intra}/k_B = -26$ K, respectively. Biradical **3** and **4** also have similar molecular and crystal structure in which J/k_B values for the intramolecular interaction were insignificant, while those for the intermolecular one were −4.85 and −37.3 K, respectively. When the magnitude of the intermolecular exchange interaction between radical centers was considered, it was found to be important to know not only the distance between radical centers but also the direction and overlap of π-orbitals occupied by radical spins.

The complex formation will be expected to make planar imidazole−radical plane by coordination of metal ions.

(14) Yoshioka, N.; Irisawa, M.; Mochizuki, Y.; Kato, T.; Inoue, H.; Ohba, S. *Chem. Lett.* **1997**, 251.
(15) Hanayama, H.; Tanaka, M.; Koga, N., unpublished result.
(16) Yamaguchi, A.; Awaga, K.; Inabe, T.; Nakamura, T.; Matsumoto, M.; Maruyama, Y., *Chem. Lett.* **1993**, 1443.

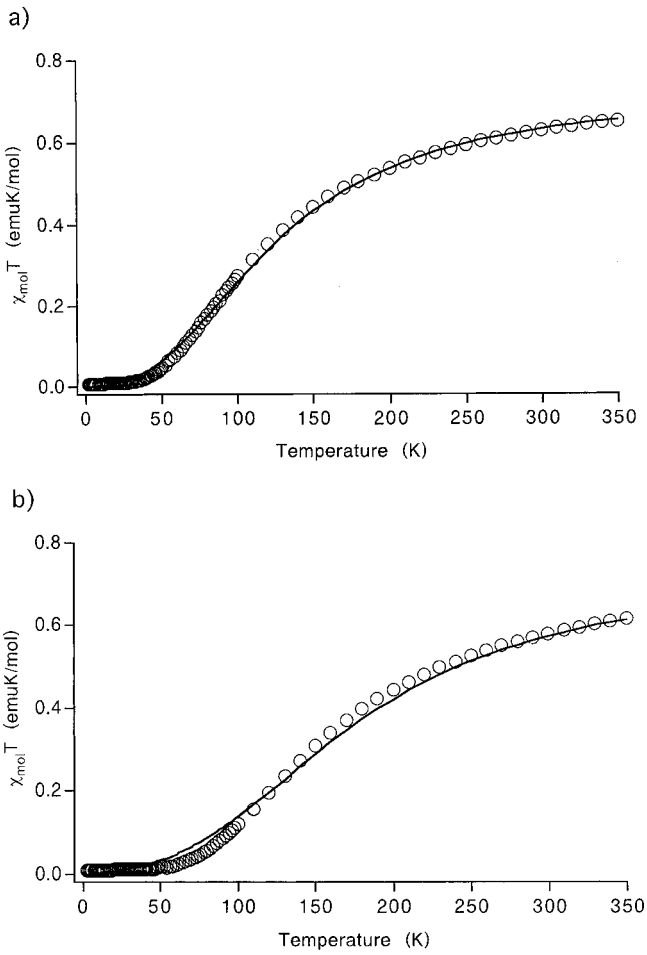

Figure 6. $\chi_{mol}T - T$ plots for **1** (a) and **2** (b). Solid curves were calculated by means of the theoretical equation[9] based on alternating linear-chain spin systems with optimized parameters.

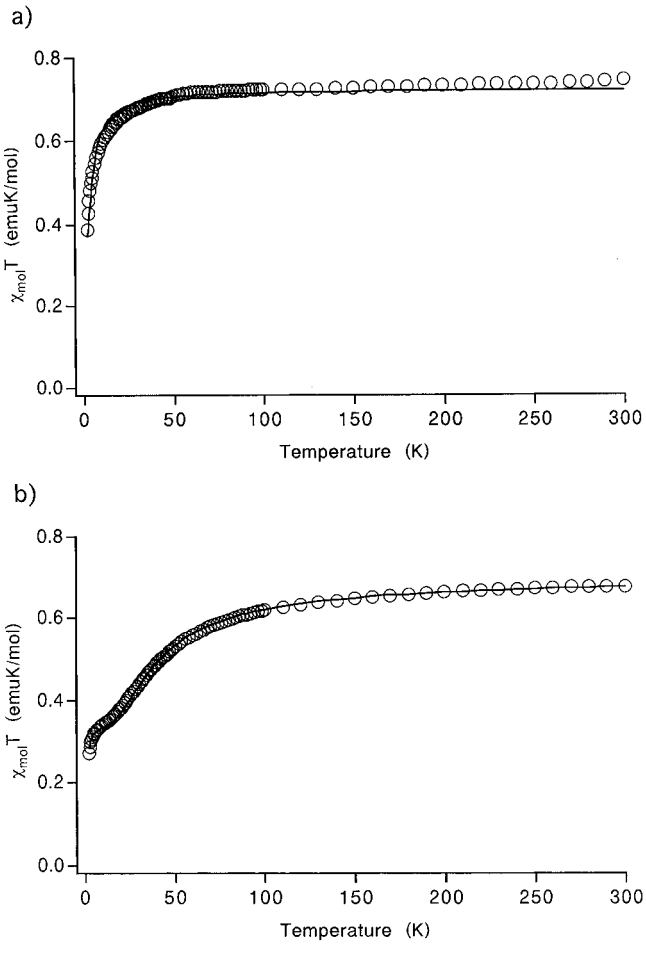

Figure 7. $\chi_{mol}T - T$ plots for **3** (a) and **4** (b). Solid curves were calculated by means of the theoretical equation based on S−T model and isolated two doublets with optimized parameters.

Efforts are underway toward preparation of magnetic metal complexes using these ligands.

Experimental Section

General Methods. Infrared spectra were recorded on a Hitachi 270-30 IR spectrometer. UV-vis spectra were recorded on a JASCO UVDEC 610C spectrometer. ^{1}H NMR spectra were measured on a JEOL 270 Fourier transform spectrometer using $CDCl_3$ as solvent and referenced to TMS. FAB mass spectra (FAB MS) were recorded on a JEOL JMS-SX102 spectrometer. Melting points were obtained with a MEL-TEMP heating block and are uncorrected. Elemental analyses were performed in the Analytical Center of Faculty of Science, Kyushu University.

X-ray Crystal and Molecular Structure Analyses. All the X-ray data were collected using Cu Kα radiation on a Rigaku AFC5R four circle diffractometer. The structures were solved in *Pbcn* for both biradical **1** and **2** in $P2_1/c$ for **3** and **4** by direct methods and refinement converged using the full-matrix least squares of the TEXAN Ver. 1.6 program (Molecular Structure Corp.). All non-hydrogen atoms were refined anisotropically; hydrogen atoms were included at standard positions (C−H 0.96 Å, C−C−H 109.5°, 120°, or 180°) and refined isotropically using a rigid model.

EPR Spectra and Magnetic Measurements. EPR spectra were recorded on a Bruker ESP 300 X-band (9.4 GHz) spectrometer equipped with a Hewlett-Packard 5350B microwave frequency counter. An Air Products LTD-3-110 liquid helium transfer system was attached for the low-temperature measurements. Sample solutions were placed in 5 mm o.d. quartz tubes, degassed by three freeze-and-thaw cycles, and sealed.

Magnetic susceptibilities were measured on Quantum Design MPMS2 and MPMS-5S SQUID susceptometers. Data were corrected for the magnetization of a sample holder and capsule used and for diamagnetic contributions which were estimated from Pascal's constants.

Materials. Unless otherwise stated, the preparative reactions were carried out under a high purity dry nitrogen atmosphere. Tetrahydrofuran (THF) and 2-methyltetrahydrofuran (MTHF) were distilled from sodium benzophenone ketyl. 2,3-Bis(hydroxyamino)-2,3-dimethylbutane was prepared by the procedure[17] reported previously. 1,3-Di-1-imidazolylbenzene and 1,3-di-1-imidazolyl-5-chlorobenzene were prepared via four steps from 1,3-diaminobenzene and 1,3-diamino-5-chlorobenzene, respectively, in a manner similar to the procedure for phenylimidazole derivatives reported by Johnson et al.[18]

1,3-Bis{1-(2-formylimidazolyl)}benzene (6). To the solution of 1.49 g (7.09 mmol) of 1,3-di-*N*-imidazolylbenzene **7** in 90 mL of anhydrous THF was added 14.6 mL of a 1.6 M solution of *n*-butyllithium in *n*-hexane at −78 °C. After stirring for 80 min, 1.81 mL (23.4 mmol) of dimethylformamide was added dropwise. The reaction mixture was stirred for 1 h at −78 °C and then left overnight at room temperature. After the usual workup, 0.97 g (3.65 mmol) of a dialdehyde **6** was obtained in 51.7% yield: mp 204−205 °C, IR (KBr) 1682 cm^{-1}, ^{1}H NMR (500 MHz, DMSO-d_6) δ 9.71 (*s*, 2H), 7.84 (*s*, 2H), 7.81 (*s*, 1H), 7.66 (*s*, 1H), 7.66 (*d*, J = 1.37 Hz, 2H), 7.46 (*d*, J = 0.69 Hz, 2H), FAB MS (*m*-nitrobenzyl alcohol): M + 1 267.

(17) Johnson, A. L.; Kauer, J. C.; Sharma, D. C.; Dorfman, R. I. *J. Med. Chem.* **1969**, *12*, 1024.
(18) Siegle, L. W.; Hass, H. B. *J. Org. Chem.* **1940**, *5*, 100.

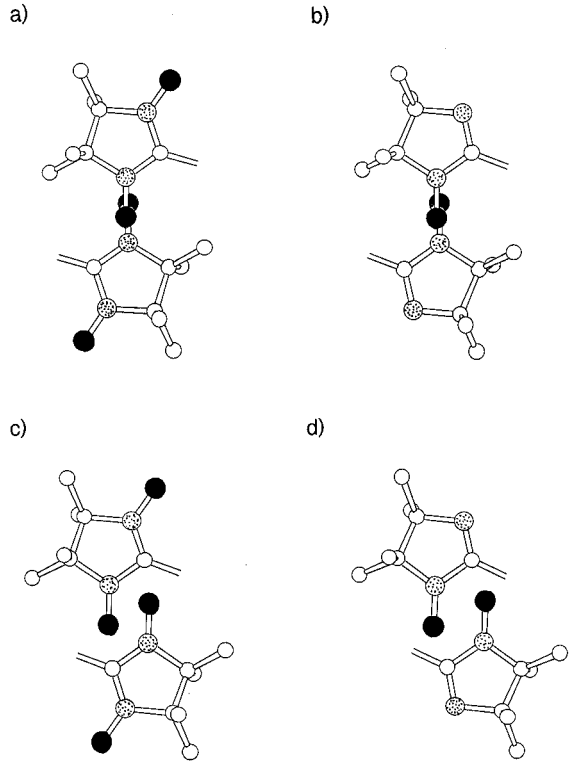

Figure 8. Ball-and-stick models for intermolecular contacts (ON−ON) of radical center units in **1** (a), **2** (b), **3** (c), and **4** (d) viewed along the direction perpendicular to ONCNO plane of a radical center. Black balls and dotted balls indicate the oxygen and nitrogen atoms, respectively.

Anal. Calcd for $C_{14}H_{10}N_4O_2$: C, 63.14; H, 3.79; N, 21.05. Found: C, 62.95; H, 3.83; N, 20.96.

1-Chloro-3,5-bis{1-(2-formylimidazolyl)}benzene (9). The compound was prepared in a manner similar to the procedure of **6** using 1-chloro-3,5-di-1-imidazolylbenzene, **10**, in place of **7**. Formyl derivative **9** was obtained in 91.8% yield: mp 204−205 °C, IR (KBr) 1698 cm^{-1}, ^1H NMR (270 MHz, $CDCl_3$) δ 9.85 (*s*, 2H), 7.50 (*d*, J = 2.02 Hz, 2H), 7.46 (*d*, J = 1.10 Hz, 2H), 7.39 (*d*, J = 0.92 Hz, 2H), 7.33 (*d*, J = 1.92 Hz, 1H), FAB MS (*m*-nitrobenzyl alcohol): M + 1 301. Anal. Calcd for $C_{14}H_{10}N_4O_2Cl\cdot{}^2/_9H_2O$: C, 55.26; H, 3.13; N, 18.42. Found: C, 55.16; H, 3.25; N, 18.28.

1,3-Bis{2-(1,3-hydroxy-4,4,5,5-tetramethylimidazolin-2-yl)imidazol-1-yl}benzene (5). To a solution of 0.58 g (2.17 mmol) of dialdehyde **6** in 30 mL of MeOH was added 1.37 g (9.30 mmol) of free 2,3-bis(hydroxyamino)-2,3-dimethylbutane. Reaction mixture was heated at 30 °C for 6 h. After the usual workup, 0.97 g (1.15 mmol) of dihydroxyamine **5** containing small amounts of the nitronyl nitroxide were obtained in 53% yield. This mixture was used for oxidation without further purification.

1-Chloro-3,5-bis{2-(1,3-hydroxy-4,4,5,5-tetramethylimidazolin-2-yl)imidazol-1-yl}benzene (8). The hydroxyamine derivative was prepared in a manner similar to the procedure of **5** using **9** in place of **6**. The mixture of hydroxyamine **8** containing the corresponding biradicals was used for the next oxidation reaction without further purification.

1,3-Bis{2-(1-oxyl-3-oxo-4,4,5,5-tetramethylimidazolin-2-yl)imidazol-1-yl}benzene (1). To a solution of 0.27 g (0.48 mmol) of **3** in 20 mL of $CHCl_3$ and 2 mL of MeOH was added 20 mL of aqueous solution of 1.02 g of $NaIO_4$ in H_2O. The suspension was stirred at room temperature for 5 min. After the usual workup, crude residue was chromatographed on aluminum oxide to afford 0.15 g (0.30 mmol) of **1** in 62% yield. Recrystallization from cyclohexane−CH_2Cl_2 gave bis(nitronyl nitroxide) **1** as a blue brick: mp 227−228 °C, UV-vis (in CH_2Cl_2) 552, 330 nm, FAB MS (*m*-nitrobenzyl alcohol matrix): 521 (M + 1, 100), 520 (69). Anal. Calcd for $C_{26}H_{32}N_8O_4$: C, 59.97; H, 6.20; N, 21.53. Found: C, 60.05; H, 6.18; N, 21.49.

1,3-Bis{2-(1-oxyl-4,4,5,5-tetramethylimidazolin-2-yl)imidazol-1-yl}benzene (2). To a solution of 0.20 g of **1** in 60 mL of CH_2Cl_2 was added 0.6 g of $NaNO_2$ in 2 mL of acetic acid. Reaction solution was stirred for 2 min at room temperature. After the usual workup, crude residue was chromatographed on silica gel to afford 0.16 g (0.33 mmol) of **1** in 85.2% yield. Recrystallization from *n*-hexane−CH_2Cl_2 gave bis(iminyl nitroxide) **2** as orange bricks: mp 228−229 °C, UV-vis (in CH_2Cl_2) 421, 330 nm, FAB MS (*m*-nitrobenzyl alcohol): 490 (M + 2, 100), 489 (57.6). Anal. Calcd for $C_{26}H_{32}N_8O_2$: C, 63.90; H, 6.61; N, 22.94. Found: C, 63.82; H, 6.56; N, 22.93.

1-Chloro-3,5-bis{2-(1-oxyl-3-oxo-4,4,5,5-tetramethylimidazolin-2-yl)imidazol-1-yl}benzene (3) and 1-Chloro-3,5-bis{2-(1-oxyl-4,4,5,5-tetramethylimidazolin-2-yl)imidazol-1-yl}benzene (4). Biradicals **3** and **4** were prepared in a manner similar to the procedure for **1** using crude **8** in place of **6**. The mixture of both radicals was chromatographed on aluminum oxide with *n*-hexane/CH_2Cl_2 as eluent to afford **3** and **4** in 16.4 and 30.2% yield, respectively. The obtained biradicals were crystallized from *n*-hexane/CH_2Cl_2/ethyl acetate and *n*-hexane/CH_2Cl_2 to give **3** and **4** as blue bricks and brown plates, respectively.

3: mp 210−211 °C. Anal. Calcd for $C_{26}H_{31}N_8O_4Cl$: C, 56.3; H, 5.64; N, 21.21. Found: C, 56.36; H, 5.69; N, 20.08.

4: mp 224−225 °C. Anal. Calcd for $C_{26}H_{31}N_8O_2Cl$: C, 59.63; H, 6.16; N, 21.41. Found: C, 59.35; H, 5.96; N, 21.16.

Acknowledgment. This work was supported by a Grant-in-Aid for Scientific Research (B) (no. 06453035) from Ministry of Education, Science and Culture, Japan. We appreciate Dr. Max Dobler of ETH who provided the program for the molecular model obtained by X-ray crystal analysis.

Supporting Information Available: Details of X-ray analysis for birdical **1**−**4** including tables of atomic coordinates, anisotropic displacement parameters, bond lengths, bond angles, torsion angles, and nonbonding contacts out to 3.60 Å (80 pages). This material is contained in libraries on microfiche, immediately follows this article in the microfilm version of the journal, and can be ordered from the ACS; see any current masthead page for ordering information.

JO971438T